Received: 18 August 2019 | Accepted: 10 February 2020

DOI: 10.1111/gcb.15079

PRIMARY RESEARCH ARTICLE

Global Change Biology WILEY

Critical land change information enhances the understanding of carbon balance in the United States

Jinxun Liu[1] | Benjamin M. Sleeter[1] | Zhiliang Zhu[1] | Thomas R. Loveland[1] | Terry Sohl[1] | Stephen M. Howard[1] | Carl H. Key[1] | Todd Hawbaker[1] | Shuguang Liu[11] | Bradley Reed[1] | Mark A. Cochrane[2] | Linda S. Heath[3] | Hong Jiang[4] | David T. Price[5] | Jing M. Chen[6] | Decheng Zhou[7] | Norman B. Bliss[1] | Tamara Wilson[1] | Jason Sherba[1] | Qiuan Zhu[8] | Yiqi Luo[9] | Benjamin Poulter[10]

[1]United States Geological Survey, USA

[2]Appalachian Laboratory, University of Maryland Center for Environmental Science, Frostburg, MD, USA

[3]USDA-Forest Service, Washington, DC, USA

[4]Nanjing University, Nanjing, China

[5]Natural Resources Canada, Edmonton, AB, Canada

[6]University of Toronto, Toronto, ON, Canada

[7]Nanjing University of Information Science and Technology, Nanjing, China

[8]Hohai University, Nanjing, China

[9]Northern Arizona University, Flagstaff, AZ, USA

[10]NASA GSFC, Greenbelt, MD, USA

[11]Central South University of Forestry and Technology, Changsha, China

Correspondence
Jinxun Liu and Benjamin M. Sleeter, United States Geological Survey, Moffett Field, CA, USA.
Email: jxliu@usgs.gov (J. L.); bsleeter@usgs.gov (B. M. S.)

Funding information
USGS Biologic Carbon Sequestration Program; DOE ALCF DD Allocation, Grant/Award Number: DE-AC02-06CH11357; USGS LANDFIRE Project; NASA Interdisciplinary Sciences, Grant/Award Number: NNX11AB89G; DOD ESTCP Program, Grant/Award Number: RC_201703

[Correction added on 8 May 2020 after first online publication: the affiliation for Shuguang Liu and affiliation 1 have been updated in this version.]

Abstract

Large-scale terrestrial carbon (C) estimating studies using methods such as atmospheric inversion, biogeochemical modeling, and field inventories have produced different results. The goal of this study was to integrate fine-scale processes including land use and land cover change into a large-scale ecosystem framework. We analyzed the terrestrial C budget of the conterminous United States from 1971 to 2015 at 1-km resolution using an enhanced dynamic global vegetation model and comprehensive land cover change data. Effects of atmospheric CO_2 fertilization, nitrogen deposition, climate, wildland fire, harvest, and land use/land cover change (LUCC) were considered. We estimate annual C losses from cropland harvest, forest clearcut and thinning, fire, and LUCC were 436.8, 117.9, 10.5, and 10.4 TgC/year, respectively. C stored in ecosystems increased from 119,494 to 127,157 TgC between 1971 and 2015, indicating a mean annual net C sink of 170.3 TgC/year. Although ecosystem net primary production increased by approximately 12.3 TgC/year, most of it was offset by increased C loss from harvest and natural disturbance and increased ecosystem respiration related to forest aging. As a result, the strength of the overall ecosystem C sink did not increase over time. Our modeled results indicate the conterminous US C sink was about 30% smaller than previous modeling studies, but converged more closely with inventory data.

KEYWORDS

carbon sequestration, DGVM, ecosystem model, ecosystem productivity, land use and land cover change, wildfire

Jinxun Liu and Benjamin M. Sleeter should be considered joint senior author.

1 | INTRODUCTION

Regionally and globally, large uncertainties exist in quantifying biological carbon (C) sequestration in terrestrial ecosystems (Arneth et al., 2017; IPCC, 2007). Atmospheric inversion models, terrestrial biogeochemical models, and field inventories typically give notably different results (Hayes et al., 2012; King et al., 2015). Grassi et al. (2018) indicated that a model–inventory discrepancy in the global anthropogenic net land use emissions (about 1.5 GtC /year) can be mostly explained by conceptual differences in dealing with forest-related land use and environmental changes. For the conterminous United States, estimates of the annual C sink during recent decades range from 200 to 685 TgC, varying greatly by method, period of analysis, and ecosystem type (Table S0-1). The recent SOCCR-2 report (Birdsey et al., 2018) indicates that estimates of the US land C sink (excluding aquatic system) are converging around 275 TgC, including 201 TgC in forestland.

Land use and land cover change (LUCC) is an important perturbation of the regional and global C cycle. Synthesis of bookkeeping models, remote sensing, and process modeling studies indicate that global LUCC-induced C emission during 1990–2009 was estimated around 1.1 PgC/year, with an overall uncertainty of ±0.5 PgC/year (Houghton et al., 2012). Several long-term global and continental scale C assessments have used process-based dynamic global vegetation models (DGVMs). Although DGVMs can reflect much greater spatial and temporal variability in C density and response to environmental conditions than bookkeeping models, their modeled C stocks may differ markedly from observations (Houghton et al., 2012). One reason is that most C cycle processes related to LUCC were simplified in large-scale C modeling assessments (Arneth et al., 2017) because DGVMs typically operate at coarse spatial resolutions with limited representation of LUCC. For example, the Community Land Model (Lindsay et al., 2014) and the Ecosystem Demography Model (Hurtt et al., 2002) have spatial resolutions of 0.5–1.0 degree for global simulations although the MC2 model has been used at 4-km resolution for western United States (Bachelet, Sheehan, Ferschweiler, & Abatzoglou, 2016). In some cases, other sources of LUCC C effects are adopted/combined in DGVM simulations (Schimel et al., 2016; Sitch et al., 2015) in order to reflect LUCC effects. In general, LUCC is represented in DGVMs at spatial resolutions which are relatively coarse compared to the spatial scales at which land cover change and land management occur (e.g., forest stands and municipal planning districts).

The conterminous United States (CONUS) has a diverse geography, comprising many ecoregions with unique biophysical and land use characteristics. The unpredictable occurrence of large wildland fires, intensive land use in forestry and agriculture, and land use change complicate attempts to assess changes in ecosystem C balance. This study integrates existing scientific knowledge, robust modeling, and the best currently available data to quantify the effects of major controlling environmental processes (atmospheric chemistry, climate variability, fire disturbance, and LUCC) on ecosystem C dynamics. The goal of this study was to include smaller scale processes such as land use and land cover in a large-scale regional ecosystem framework. Our approach evaluates C sequestration in dominant vegetation types (forests, shrublands, grasslands, croplands) in CONUS from 1971 to 2015 at 1-km resolution by reconciling a modeling approach with county-scale observations. The study focuses on changes in ecosystem productivity, C storage, and biomass C losses from disturbances. Our modeling tool and various model input data are described in Section 2 and Supporting Information.

Significance

Differences in input data and methods cause discrepancies in large regional carbon (C) assessment results. C sequestration estimates from bottom-up ecosystem models are usually smaller than estimates from atmospheric inversion models and larger than field inventory results. Here, we quantify C dynamics of the conterminous United States at 1-km spatial resolution focusing on detailed land cover changes over recent decades, using several proven and established national data products. Our research highlights that the combined impacts of land management, human-dependent land use change, and natural disturbance on C are greater than those associated with climate variability, and that process modeling can converge with field inventory data when detailed land cover change information is used.

2 | METHODS

2.1 | Model description

The Integrated Biosphere Simulator (IBIS; Foley et al., 1996) is a DGVM that links mesoscale atmospheric drivers and vegetation ecophysiology in a physically consistent representation of canopy photosynthesis and stomatal conductance, while accounting for vegetation phenology and soil biogeochemistry to simulate long-term vegetation dynamics and ecosystem productivity. IBIS allows multiple plant functional types (PFTs; see Table S0-3) to coexist in a single land pixel. Existence of a PFT depends on local-scale environmental conditions and is constrained by human land use. IBIS does not directly use forest age to calculate forest growth. Each forest PFT within a grid cell contains a single biomass C density. The biomass density together with the climate and disturbance variables determine the PFTs growth and mortality rates.

In this study, our modified version of IBIS introduces detailed effects of land cover change, wildland fire, forest thinning, and cropland grain/straw harvest (Liu et al., 2016). The model was enhanced to use comprehensive gridded LUCC data. The model handles eight

major land transitions/disturbances (fire, forest clearcut, forest thinning, deforestation to other vegetation, reforestation from other vegetation, agricultural expansion from grassland, agricultural contraction to grassland, and urban/infrastructure development). C transfer following LUCC and fire events includes direct C harvest/combustion and additional vegetation mortality.

The modified IBIS model incorporates fractional land cover changes. Each 1-km grid cell contains multiple land cover types. Each land cover type (e.g., forest, grass and agriculture) can have multiple PFTs (see Table S0-3). Each PFT has a single set of biomass pools and fluxes. The IBIS model does not consider forest age directly. It uses biomass C density to adjust new biomass growth and mortality.

Forest thinning in a grid cell is determined by an external thinning ratio derived from the USDA Forest Service Forest Inventory and Analysis (FIA) and literature, which applies to entire forest PFTs annually. All live biomass from forest PFTs will be reduced following the thinning ratio. More details are presented in the Supporting Information.

2.2 | Key input data

In this study, IBIS was enhanced to use comprehensive LUCC data: (a) 30-m vegetation height and cover type information from the USDA-USGS LANDFIRE Program; (b) five dates (1973, 1979, 1986, 1992, 2000) of 60-m resolution land cover change information from the USGS Land Cover Trends Project; (c) 30-m resolution annual wildland fire scar and burn severity information (1984–2015) from the USGS-USDA Monitoring Trends in Burn Severity (MTBS) Project; and (d) freshwater and saline wetland area fractions derived from 30-m National Land Cover Database (NLCD) and NOAA Coastal Change Analysis Program data. These publicly available datasets for CONUS are the largest and most comprehensive of their kind. In addition, state/county-level forest thinning rates were derived from previous studies (Law, Hudiburg, & Luyssaert, 2013; Zhou, Liu, Oeding, & Zhao, 2013).

To better constrain the model's prognostic representation of the C cycle at regional scales, we used region-specific C densities as calibration references for each county in CONUS. MODIS-derived annual net primary productivity (NPP) from 2001 to 2005 (Zhao, Heinsch, Nemani, & Running, 2005), forest live biomass and dead wood standing stock at 100 years from the Carbon On Line Estimator (COLE) tool (Van Deusen & Heath, 2016), and USDA NASS county-level crop harvest data (https://www.quickstats.nass.usda.gov/) were used to calibrate the model. The COLE tool is based on USDA Forest Service FIA data (USDA Forest Service, 2016; http://fia.fed.us), which is also used in development of LANDFIRE and some NLCD mapped products. Details are provided in Section 2 and Supporting Materials.

Details of LUCC-related data are provided in Supporting Materials S1, S2, S3, and S4. Table S0-2 provides key data links. Dynamic monthly precipitation and temperature data from 1971 to 2015, interpolated to 4-km resolution using PRISM (Daly et al., 2008), were used as the main climatic drivers. Other variables like monthly mean cloud cover fraction, wet days per month, relative humidity, and wind speed were adopted from monthly normals for 1961–1990 obtained from the UK Climate Research Unit (http://www.cru.uea.ac.uk/). The soil texture and C content were obtained from SSURGO (2015) polygon data and reprocessed/interpolated to 1-km resolution. The modeled soil profiles contain up to six layers (0–7, 7–15, 15–25, 25–50, 50–100, and 100–200 cm). Sand, silt, and clay fractions of each layer are used by IBIS to calculate soil water holding capacity and permeability. Additionally, 0.5-degree spatially explicit seasonal surface CO_2 concentration (2003–2009) and annual nitrogen deposition (1970–2009) were derived from satellite-based column density measurements (Lu et al., 2016; Zhang et al., 2014). The 1-km land ownership map was derived from the Protected Areas Database of the United States, version 1.4 (USGS, 2016).

2.3 | Consideration of fractional land cover

IBIS tracks annual changes in the area fractions of each land cover type within each land pixel. The original IBIS model simulated the existence of each PFT using climatic constraints only, which could give very different upper and lower canopy fractions from reality in regions where human activities have a major influence and in regions where physical limitations on vegetation exist (such as rock, desert, or open water). In our modified version, observed fractional land cover data are used to constrain the extent of changes in LAI and the proportions of different PFTs. Land cover fractions, including the unvegetated fraction, are not allowed to change unless a relevant LUCC event occurs.

Vegetation regrowth occurs following any disturbance or human-caused land use change. Disturbance applies to an entire PFT and land cover type in the model. When wildfire and forest harvest events occur (which are not permanent land cover conversions), the forest fraction will remain unchanged, with only biomass density (kgC/m^2) being reduced; however, when deforestation occurs, all of the forest fraction will be converted to the target land cover (e.g. agricultural land, grassland, shrubland, etc.) except that we intentionally allow a small fraction (5%) of forest to exist during urbanization. Conversely, when reforestation/afforestation occurs, either natural or human induced, other land covers convert to forest, causing the forestland fraction to increase, although the forest biomass density of the entire grid cell may not immediately increase. Following LUCC events, different proportions of ecosystem C will transfer to the atmosphere, harvest products, and on-site dead wood.

2.4 | Forest biomass and soil carbon initialization

We used a county-level scalar and retrospective cold-start simulations (i.e., forest biomass starts from zero) to obtain county-level average forest standing stocks at 100 years that matched with FIA-COLE observations (per hectare biomass densities). For individual forest pixels in a county, we assumed that the pixel-level forest growth rates varied around the county mean forest growth rate. The variability is driven by local environmental factors specific to its soil,

climate, tree cover fraction, and PFTs. When forest area fraction changes, pixel-level ecosystem production and biomass values will change based on the new forest area fraction. Based on those pixel-level biomass-over-age growth curves, we used the "observed" 1-km forest biomass map generated from LANDFIRE data (Supporting Material S1) to determine the approximate forest age in 2000 and reconstructed the age and biomass for 1971. For a pixel where biomass derived from LANDFIRE was larger than that simulated by IBIS at 100 years, we assumed the forest was mature and used the LANDFIRE estimate as its biomass in 1971. For a pixel where forest age backtracking indicated a stand-replacing disturbance occurred between 1971 and 2000, we assumed the previously disturbed forest was mature and set the biomass in 1971 to that of a forest with an age selected at random between 30 and 100 years. This assumption could lead to slightly lower estimates of wood harvest for the western old-growth forest and slightly higher estimates of harvest for the southeastern plantations.

Initialization of soil C pools was based on soil survey data (Soil Survey Staff, 2019). Soil C has four pools: fast, unprotected slow, protected slow, and passive. These pools are not further divided by soil layers. IBIS soil layers are mainly used for water balance calculation. Our soil C calculation in the first 10 years was similar to the fast soil spin-up method of Xia, Luo, Wang, Weng, and Hararuk (2012), which compared input and output fluxes of total soil C. When input and output fluxes became very close, the soil C pool was close to a theoretical balanced state. To maintain the overall soil C pool size close to observations, we used a set of internal scalars in the first 20 simulation years that dynamically adjust the slow soil C pool size and then deducted the slow C from the total observed soil C to obtain the size of the initial passive soil C pool. To avoid drastic declines of soil C in the simulation, we used an approach similar to the LPJ-WHy model (Wania, Ross, & Prentice, 2009) in modeling peatland soil accumulation: A maximum amount of the passive soil C (reactive, 5 kg C/m^2) is allowed to participate in the soil decomposition process. The extra passive soil C (beyond 5 kg C/m^2) is assumed inactive within a given year. IBIS has ground litter C and dead wood C pools in addition to the four soil C pools. Dead wood calibration was done using FIA-COLE county-level 100-year dead wood data (same as live biomass calibration). Ground fine litter was calculated with IBIS default litter decomposition parameters.

2.5 | Model calibration

Model calibrations were performed by comparing simulated county-level NPP, live biomass, dead wood, and crop yield with county-level observations of MODIS-derived NPP, FIA-derived forest live biomass, dead wood, and USDA statistics of crop yields (Figure S5-1).

The COLE tool provides 100-year forest growth curves (live and dead wood) based on FIA data for each FIA survey unit (Table S5-1; Figure S5-1). It was assumed that a 100-year-old forest did not undergo any stand-replacing disturbances, although effects of thinning, non–stand-killing fires or other disturbances are implicitly included in the FIA data. Repeated IBIS simulations were performed with disturbance events turned off and compared with the COLE-based FIA data. Scaling coefficients for each county were then calculated and applied to adjust IBIS' simulations of forest live growth and dead wood. County-level live biomass scaling coefficient was calculated as a ratio of simulated county-level 100-year forest biomass over FIA-derived county-level 100-year forest biomass. The ratio was constrained between 0.1 and 10.0 and applied to tree mortality calculation in the next simulation. Repeated adjustments helped to make the simulation and observation converge. Dead wood scaling coefficient was calculated the same way using dead wood data.

We summarized county-level annual agricultural harvest data (comprising 26 crop species) since 1960. The yield data were aggregated based on their area fractions (Table S5-2). The 2000–2009 averages were used to calibrate IBIS agricultural harvest amounts over the same period. The 1960–2009 grain yield trend was used to adjust grain production increase in addition to simulated effects of CO_2 fertilization.

The MODIS-derived NPP product provided full spatial and temporal coverage, which was used to calibrate IBIS NPP at the ecoregion level. IBIS does not consider individual tree/crop species and other local management factors that would be captured by remote sensing. We avoided overfitting because IBIS has its own NPP algorithm. Although this was not a pixel-level calibration, simulated NPP would still respond to spatial variability driven by climate, soil, and disturbance on the 960-m grid.

Four uncertainty statistics methods were used to evaluate model performance, including Pearson correlation coefficient, root mean square error, modeling efficiency, and mean relative difference. Details are provided in Supporting Material S5.

3 | RESULTS

3.1 | Land cover transition and related carbon gains and removals

Over the study period, wildland fire and forest clearcut disturbed the most land area, followed by agricultural contraction and expansion, development, and forest to/from agricultural land (Table 1).

The mean annual C loss was 572.6 TgC/year, including grain harvest (284.5), straw harvest (152.3), forest clearcut harvest (31.9), forest thinning (86.0), direct emissions from fires (10.5), and C losses related to other land transitions (10.4). These C losses were partly compensated by vegetation regrowth. For example, over the 45 years, average total net biome productivity (NBP; negative values denote C loss) of all clearcut harvest sites was −14.0 TgC/year, whereas the average annual C removal on clearcut sites was 31.9 TgC/year. Similarly, all wildfire sites together sequestered 5.5 TgC/year, while their average annual C loss in combustion was 10.5 TgC/year. Fire emission was not available before 1984 due to lack of wildfire data. This would cause underestimation of C loss in those years. The underestimation might be close to the average annual fire emissions during 1984–1990 (6

TABLE 1 Land cover change and fire effects on ecosystem carbon fluxes in CONUS (1971–2015 average NPP and NBP). The areas are the sum of the land pixels that had undergone the same LUCC events during 1971–2015. A positive NBP value refers to a net carbon sink on land. Fire disturbance locations overlap with the No-LUCC locations. The land area and carbon numbers on the No_LUCC row already include the numbers from the Fire row. Therefore, the numbers on the Sum/Avg row do not include the numbers from the Fire row. The fire area included 14,000+ fires from 1984 to 2015. No fire data were available from 1971 to 1983. Forest thinning was assumed to occur across all forested areas annually

Change type	AREA (km^2)	NPP ($kgC\ m^{-2}\ year^{-1}$)	NPP_SUM (TgC/year)	NEP ($kgC\ m^{-2}\ year^{-1}$)	NEP_SUM (TgC/year)	NBP ($kgC\ m^{-2}\ year^{-1}$)	NBP_SUM (TgC/year)
No_LUCC	6,835,273	0.36	2,480.7	0.10	665.5	0.027	182.9
Fire	547,034	0.33	181.5	0.04	23.4	0.010	5.5
Forest clearcut harvest	316,501	0.55	175.2	0.09	28.5	−0.044	−14.0
Deforestation to Ag.	39,515	0.43	16.9	0.16	6.1	−0.030	−1.2
Reforestation from Ag.	38,512	0.61	23.5	0.15	5.8	0.065	2.5
Forest to development	38,735	0.38	14.8	0.09	3.4	−0.023	−0.9
Grass to development	15,702	0.18	2.8	0.04	0.7	−0.019	−0.3
Ag. to development	50,164	0.27	13.8	0.09	4.5	−0.021	−1.1
Ag. expansion from grass	123,993	0.30	37.3	0.16	20.2	−0.004	−0.5
Ag. contraction to grass	183,977	0.28	51.0	0.04	8.1	0.015	2.8
Sum/Avg (excluding fire row)	7,642,373	0.368	2,816	0.097	743	0.022	170

Abbreviations: LUCC, land use and land cover change; NBP, net biome productivity; NEP, net ecosystem productivity; NPP, net primary productivity.

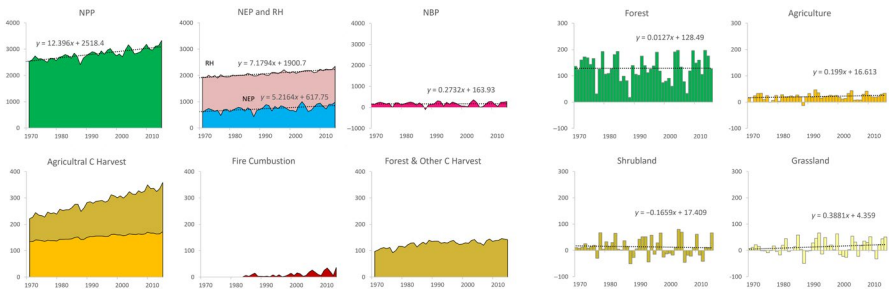

FIGURE 1 Temporal trends of major carbon fluxes of CONUS from 1971 to 2015. Units are TgC/year. A positive NBP value refers to a net carbon sink on land. NBP, net biome productivity; NEP, net ecosystem productivity; NPP, net primary productivity; RH, ecosystem heterotrophic respiration

TgC/year), which was lower than the fire emissions during 2011–2015 (25 TgC/year). Urban development areas on average lost 2.3 TgC/year. Areas with unchanged land cover sequestered 182.9 TgC/year.

3.2 | Carbon trends and spatial distribution

Figure 1 shows the simulated trends in key ecosystem C fluxes and stocks from 1971 to 2015. Due to the combined contributions of CO_2 fertilization, plant phenology, climate change, and land change impacts, average NPP increased by about 23% during 1971–2015 (18.5% in forests, 7% in shrubland, 27.9% in grassland, and 31.7% in agricultural systems), calculated using the linear trend line of the 45-year NPP values. NPP of agricultural land had the highest increase partly due to farming and biotechnology advances, which were represented in the model empirically, based on 1960–2010 crop yield data. Average total NBP was 170 TgC/year, ranging from a loss of 104 TgC/year in 1988 to a maximum uptake of 366 TgC/year in 2004. Clearcut harvest removals averaged 32 TgC/year and were lowest in the 1970s (21 TgC/year) and highest in the late 1980s (36 TgC/year), whereas forest thinning removed approximately 86 TgC/year. Combustion of soil and biomass C was 6 TgC/year during 1984–2000, but increased to 12 TgC/year in 2000s, and reached 25 TgC/year during 2001–2015, with large interannual variation. C losses in agricultural harvests (grain + straw) increased steadily from 374 TgC/year to 505 TgC/year over the simulation period. Total C increases in live biomass, dead wood, other plant litter, and soil were 4.19, 1.16, 0.57, and 1.75 PgC, respectively. More than half of the C stock increase was in live biomass (55%), followed by soil (23%), dead wood (15%), and litter (7%).

Summaries of C stocks and fluxes by land cover class and by decade from 1971 to 2015 are listed in Table 2. Overall, the estimated CONUS terrestrial ecosystem C sink of 170 TgC/year (not including C sink in aquatic systems and harvested wood product) offset about 11.5% of total CONUS fossil fuel emissions (1,476 TgC/year) (King et al., 2015). The highest decadal NBP occurred in the 1990s (188 TgC/year), due to favorable climate and relatively small areas disturbed. However, NBP was low in the 2000s (166 TgC/year), when C removals in agriculture, fire disturbances, and LUCC increased. The average NBP of 2011–2015 recovered to 192 TgC/year.

TABLE 2 Overall carbon fluxes and stocks in CONUS by land cover type and by decade. Flux values by land cover are the 1971–2015 averages. Stock values by land cover are for 2015. The "Other" lands include all lands in CONUS with non-vegetation cover of greater than 85%, mostly barren, and urban areas. Area unit is km^2; C stock unit is TgC; C flux (NPP, NEP, NBP) unit is TgC/year

	Area (1971)	Area (2015)	NPP	NEP	NBP	Live Biom C	Dead Biom C	Litter C	Soil C	Total C
Forest	2,737,374	2,709,645	1,448	280	129	15,407	2,374	3,454	40,461	61,695
Crop	2,018,467	1,958,302	747	395	21	1,875	208	696	28,429	31,209
Shrub	1,670,473	1,651,758	282	28	14	1,051	428	723	11,004	13,206
Grass	1,174,161	1,185,146	325	35	14	624	104	638	14,727	16,094
WdCrop	10,066	10,066	7.6	5.1	0.1	22	0	6	104	132
Other	31,833	127,456	7.8	0.9	−7.6	63	8.0	16.4	947	1,034
Sum	7,642,374	7,642,374	2,817	744	170	19,043	3,123	5,533	95,672	123,371
1970s			2,607	653	171	17,488	2,676	5,277	95,041	120,482
1980s			2,698	686	145	18,559	2,948	5,378	95,265	122,150
1990s			2,868	776	188	19,354	3,174	5,605	95,671	123,804
2000s			2,947	796	166	19,984	3,430	5,701	96,227	125,342
2010s			3,105	866	192	20,543	3,630	5,865	96,645	126,683
AVG 71-15			2,816	743	170	19,035	3,121	5,532	95,673	123,360

Abbreviations: NBP, net biome productivity; NEP, net ecosystem productivity; NPP, net primary productivity.

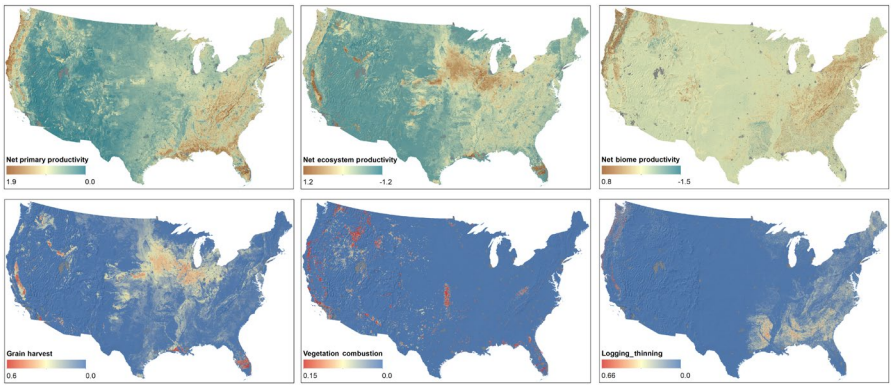

FIGURE 2 Spatial distribution of 45-year average net primary productivity (NPP), net ecosystem productivity (NEP), net biome productivity (NBP), and carbon losses from grain harvest, tree harvest, and fire. Unit is kgC m^{-2} $year^{-1}$

Figure 2 shows the spatial patterns of ecosystem NPP, net ecosystem productivity (NEP), NBP, and C removals from fire and harvest averaged over the 45-year simulation period. The US west coast and the eastern United States had generally high NPP and NBP, mostly in forested regions. Agricultural land had the highest NEP and medium high NPP, but its NBP was low due to grain and straw removals.

4 | DISCUSSION

4.1 | Implications for LUCC-based C modeling

Our study provides a number of important insights on the quantification of LUCC and fire effects on CONUS C cycling. First, the interannual variations in NPP and NEP were driven mainly by climate variability without counting LUCC and fire effects. In our study, LUCC and fire disturbance caused C loss of approximately 573 TgC (STD = 68 TgC) per year on average (including 437 TgC/year loss from agricultural land), which offset 77% of total NEP (743 TgC/year). This huge C loss greatly exceeded year-to-year variability (STD) in NPP (199 TgC/year), NEP (121 TgC/year), and NBP (96 TgC/year). If we look at forestlands only, C losses caused by clearcut and thinning (104 TgC/year, STD = 13.2 TgC/year) also exceeded the variations of forest NPP (93 TgC/year), NEP (53 TgC/year), and NBP (47 TgC/year). This demonstrates that human land use and natural disturbance are key factors in the C balances of the CONUS ecosystems, with larger magnitude and smaller variation than climate variability effects.

Second, most terrestrial C sinks occur in areas unaffected by LUCC, primarily on forestlands, with about 55% of the C sink allocated to living biomass. Although forest NPP and NEP increased by 18.5% and 33.4%, respectively, forest NBP basically remained the same during the study period. This leveled NBP of forest was attributable to a combination of increased C gain from NPP and increased C loss from heterotrophic respiration, LUCC, and fire disturbances.

Third, our estimates are generally more consistent with results from inventory-based methods, which consistently estimate a

smaller land C sink than ecosystem models and atmospheric inversion methods (Table S0-1). Simulated forestland C sink in the 1990s was 125 TgC/year. If we consider an estimated 25 TgC/year sink in harvested wood products (Pan et al., 2011; U.S. Environmental Protection Agency, 2014), our adjusted 1990s forest NBP estimate would be 150 TgC/year. Because our forest summary included only land cells where forest cover was dominant, and because we used fractional land cover in the model, a portion of the C sink in shrublands, grasslands, and agricultural lands (total about 63 TgC/year) could be attributed to additional C uptake by trees. Our statistics indicate that average tree biomass density on forestland, agricultural land, shrubland, and grassland during 1971–2015 was 5.60, 0.81, 0.16, and 0.20 kg C/m^2, respectively. Therefore, about 14.5% of agricultural lands, 2.9% of shrubland, and 3.6% of grassland can be considered tree-covered land. That equals approximately 13.9% of normal forestland area. Therefore, given a forestland C sink of 125 TgC/year in 1990s, we can assume an additional C sink of 17 TgC/year for forests in non-forest dominant lands. Sparse trees on agricultural land usually have higher productivity than trees in a forest stand due to better soil nitrogen and water supply and edge effect. But sparse trees on non-agricultural lands may reside in a harsh environment (such as cold mountaintop) and have lower productivity than normal forest. Given that we have more than doubled sparse tree areas on agricultural land than on shrubland and grassland, we think the additional 17 TgC/year C sink is conservative and reasonable. Our new adjusted forest NBP estimate for the 1990s would be 167 TgC/year, which is very close to some forest inventory studies, such as Pan et al. (2011; 179 TgC/year), Heath, Smith, Skog, Nowak, and Woodall (2011; 162 TgC/year), and Woodbury, Smith, and Heath (2007; 169 TgC/year). For the 2000s, our adjusted estimate of forest NBP (with dynamic climate data used) is still 167 TgC/year. This value is a little lower than the inventory-based forest NBP (199 TgC/year) that usually has limited response to climate variability. However, our estimate of 2011–2015 forest C sink is 195 TgC/year, which is close to inventory results. On the contrary, our adjusted average NBP on all land types for 1991–2010 was 202 TgC/year, which is significantly lower than that obtained from other models (average of 331 TgC/year) and the SOCCR2 NBP estimates (275 TgC/year).

Our model's agreement with forest inventory estimates (1990s) may be partially explained by our calibration of modeled live biomass C stock and dead woody C stock against surveyed county-level 100-year-old forest stands. However, our calibration was done before fire and LUCC data were used. Therefore, our LUCC-related C budget is mostly independent from an inventory-based C budget. Our regional model calibration approach is likely the big difference from the site-level calibration approach used by other DGVM models. Additionally, our model considered land ownership, by which public or protected lands (mostly in the western United States) have reduced thinning rates compared to private lands (mostly managed land in the eastern United States). Overall, our findings represent the most comprehensive C modeling exercise utilizing available LUCC data for CONUS. Results indicate that combined effects of direct management, human-caused LUCC, and natural disturbance on C budget are larger than those associated with climate variability. However, we acknowledge that natural disturbances (such as wildland fires) also vary with climate. So additional work is needed to understand the full influence of climate variability.

Using a bookkeeping modeling approach, Piao et al. (2018) found that lower land use emissions were responsible for the global increased land C sink since the 2000s. From our study, overall LUCC-induced total biomass removals (beyond fire emission) gradually increased, with the 2000–2009 period being slightly lower than the 1990s and the 2010–2015 period, which is consistent with the global trend. Land conversions had relatively higher C emissions (biomass removals) during 1985–2000, and logging reached the highest level during late 1980s and early 1990s. But CONUS wildland fires significantly intensified since the 2000s.

Pugh et al. (2019) pointed out that age-related forest C sink is predominantly located in the middle latitudes. Although IBIS does not track forest age, our study seems to support that statement. From our study, IBIS showed significant increases in forest NPP and sustained NBP level even with gradually increased biomass removals and fire combustions. Our initial analysis indicated that, after excluding climate effects, forest NPP increased by 17% during 1971–2015. Considering this NPP increase, the model can generate 100-year total tree biomass that matches the 100-year biomass level derived from inventory. We believe the driving forces behind the NPP increase are the CO_2 enrichment effect and forest age effect. Currently, although the IBIS model's photosynthesis formula includes a conservative CO_2 fertilization algorithm, we cannot separate the contributions of the two factors effectively. Further work is needed to quantify the relative contributions of forest age and CO_2 fertilization.

4.2 | Reducing model uncertainties

Many aspects of this study still have notable uncertainties. First, dead wood C is one of the big unknowns in C modeling. In this study, although we calibrated our model with surveyed overall forest dead wood C stock at 100 years, we still do not have good dead wood C initialization. In addition, we did not explicitly model the effects of insects, disease, and physical agents such as flooding on tree mortality. Adding greater details to the tree mortality process, including the transfer of live tree C to dead tree C and the temporal changes in decomposition rates of standing and downed dead wood pools (Landry, Parrott, Price, Ramankutty, & Matthews, 2016; Landry, Price, Ramankutty, Parrott, & Matthews, 2016), would improve NBP calculations in future work. Second, although total C removal from forests (including clearcut, thinning, and other deforestation events) was about 128 TgC/year, which matched inventory-based estimates (Williams, Gu, MacLean, Masek, & Collatz, 2016), thinning practices by region and by ownership across CONUS are still highly uncertain, especially in the interior western United States. Separation of partial thinning and

clearcut can be further improved when better annual clearcut data become available. Third, estimates of annual land area burned also have considerable uncertainty. By mapping fires from 1984 to 2015 using Landsat data, Hawbaker et al. (2017) found 31% more area burned than reported in MTBS in the western United States, 312% more in the Great Plains, and 233% more in the eastern United States. Therefore, the apparently low C removals due to fire may be attributed to the focus of the MTBS database on large fires (defined as 1,000 acres in the west and 500 acres in the eastern United States). Finally, given that spatially explicit and comprehensive historical land change data were not available, we generated annual wall-to-wall land cover maps (1971–2015) based on land cover change sampling. The overall accuracy of land cover change sampling was reported to be 85% (USGS Land Cover Trends Project). Yet, new approaches, including annual wall-to-wall remote sensing products (e.g., USGS Land Change Monitoring, Assessment, and Projection project) and robust land cover change models will be very helpful to reconstruct more realistic land cover and biomass histories. In addition, DGVMs that can deal with fractional land cover change will be useful for large-scale, coarse resolution regional and global simulations. This feature of our model allows direct use of future land cover products such as the harmonized land use projections (Hurtt et al., 2011) developed for the IPCC's Fifth Assessment Report.

ACKNOWLEDGEMENTS

This study was supported by the USGS Biologic Carbon Sequestration Program (LandCarbon). Early funding for this work was also provided by the NASA Interdisciplinary Sciences (NNX11AB89G) and USGS LANDFIRE projects. Additional funding also includes the DOD ESTCP Program (RC_201703). We thank the researchers from the USGS Land Cover Trends project and the MTBS project for data and technical assistance. Xiaomeng Huang, Jie Yang, and Wanjing Wei from Qinghua University and Thomas Uram from Argonne National Laboratory helped with parallel IBIS I/O development. Zhen Zhang from University of Maryland provided monthly spatial CO_2 data and Xuehe Lu of Nanjing University provided annual nitrogen deposition data. Carol Deering assisted in reference searches and citations. Thomas Adamson conducted a technical edit. This research used resources of the Argonne Leadership Computing Facility, which is a DOE Office of Science User Facility supported under Contract DE-AC02-06CH11357.

CONFLICT OF INTEREST

The authors have no conflict of interest to declare.

AUTHOR CONTRIBUTIONS

J.L. and B.M.S. have equal contributions to this work. J.L. and Q.Z. carried out the IBIS modeling work. B.M.S., T.R.L., T.S., and T.W. carried out the land cover change analysis. S.M.H., C.H.K., and T.H. carried out fire data analysis. Z.Z. and B.R. were involved in the whole study design with J.L. and B.M.S. L.S.H. guided the understanding and use of the COLE database. D.Z. helped with forest thinning quantification. N.B.B. processed the SSURGO soil data. J.S. contributed to data archiving. S.L., M.A.C., H.J., D.T.P., J.M.C., Y.L., and B.P. contributed to carbon modeling and/or carbon analysis in many aspects. All authors contributed to and approved the final manuscript.

DATA AVAILABILITY STATEMENT

Spatial input and output data supporting the conclusions of the study are available through the USGS ScienceBase repository. The parallel IBIS model code, including parameter files are available from the corresponding authors and also available on Github: https://github.com/jxliu2018/pIBIS.

ORCID

Jinxun Liu https://orcid.org/0000-0003-0561-8988
Benjamin M. Sleeter https://orcid.org/0000-0003-2371-9571
Yiqi Luo https://orcid.org/0000-0002-4556-0218
Benjamin Poulter https://orcid.org/0000-0002-9493-8600

REFERENCES

Addiscott, T., & Whitmore, A. (1987). Computer simulation of changes in soil mineral nitrogen and crop nitrogen during autumn, winter and spring. *The Journal of Agricultural Science*, *109*, 141–157. https://doi.org/10.1017/S0021859600081089

Arneth, A., Sitch, S., Pongratz, J., Stocker, B. D., Ciais, P., Poulter, B., … Zaehle, S. (2017). Historical carbon dioxide emissions caused by land-use changes are possibly larger than assumed. *Nature Geoscience*, *10*, 79–84. https://doi.org/10.1038/NGEO2882

Bachelet, D., Sheehan, T., Ferschweiler, K., & Abatzoglou, J. (2016). Simulating vegetation change, carbon cycling, and fire over the western United States using CMIP5 climate projections. In K. Riley, P. Webley, & M. Thompson (Eds.), *Natural hazard uncertainty assessment: Modeling and decision support* (pp. 257–275). Hoboken, NJ: John Wiley & Sons, Inc. https://doi.org/10.1002/9781119028116.ch17

Birdsey, R., Mayes, M. A., Romero-Lankao, P., Najjar, R. G., Reed, S. C., Cavallaro, N., … Zhu, Z. (2018). Executive summary. In N. Cavallaro, G. Shrestha, R. Birdsey, M. A. Mayes, R. G. Najjar, S. C. Reed, P. Romero-Lankao, & Z. Zhu (Eds.), *Second State of the Carbon Cycle Report (SOCCR2): A sustained assessment report* (pp. 21–40). Washington, DC: U.S. Global Change Research Program. https://doi.org/10.7930/SOCCR2.2018.ES

Daly, C., Halbleib, M., Smith, J. I., Gibson, W. P., Doggett, M. K., Taylor, G. H., … Pasteris, P. P. (2008). Physiographically-sensitive mapping of climatological temperature and precipitation across the conterminous United States. *International Journal of Climatology*, *28*, 2031–2064. https://doi.org/10.1002/joc.1688

Foley, J. A., Prentice, I. C., Ramankutty, N., Levis, S., Pollard, D., Sitch, S., & Haxeltine, A. (1996). An integrated biosphere model of land surface processes, terrestrial carbon balance, and vegetation dynamics. *Global Biogeochemical Cycles*, *10*, 603–628. https://doi.org/10.1029/96GB02692

Grassi, G., House, J. O., Kurz, W. A., Cescatti, A., Houghton, R. A., Peters, G. P., … Zaehle, S. (2018). Reconciling global-model estimates and country reporting of anthropogenic forest CO_2 sinks. *Nature Climate Change*, *8*, 914–920. https://doi.org/10.1038/s41558-018-0283-x

Hawbaker, T. J., Vanderhoof, M. K., Beal, Y.-J., Takacs, J. D., Schmidt, G. L., Falgout, J. T., … Dwyer, J. L. (2017). Mapping burned areas using dense time-series of Landsat data. *Remote Sensing of Environment*, *198*, 504–522. https://doi.org/10.1016/j.rse.2017.06.027

Hayes, D. J., Turner, D. P., Stinson, G., McGuire, A. D., Wei, Y., West, T. O., … Cook, R. B. (2012). Reconciling estimates of the contemporary North American carbon balance among terrestrial biosphere models, atmospheric inversions, and a new approach for estimating net ecosystem exchange from inventory-based data. *Global Change Biology*, *18*, 1282–1299. https://doi.org/10.1111/j.1365-2486.2011.02627.x

Heath, L. S., Smith, J. E., Skog, K., Nowak, D., & Woodall, C. (2011). Managed forest carbon estimates for the U.S. Greenhouse Gas Inventory, 1990–2008. *Journal of Forestry*, *2011*(April/May), 167–173.

Houghton, R. A., House, J. I., Pongratz, J., van der Werf, G. R., DeFries, R. S., Hansen, M. C., … Ramankutty, N. (2012). Carbon emissions from land use and land-cover change. *Biogeosciences*, *9*, 5125–5142. https://doi.org/10.1093/jof/109.3.167

Hurtt, G. C., Chini, L. P., Frolking, S., Betts, R. A., Fischer, G., Hibbard, K., … Wang, P. (2011). Harmonization of land-use scenarios for the period 1500–2100: 600 years of global gridded annual land-use transitions, wood harvest, and resulting secondary lands. *Climatic Change*, *109*, 117–161. https://doi.org/10.1007/s10584-011-0153-2

Hurtt, G. C., Pacala, S. W., Moorcroft, P. R., Caspersen, J., Shevliakova, E., Houghton, R. A., … Moore III, B. (2002). Projecting the future of the U.S. carbon sink. *Proceedings of the National Academy of Sciences of the United States of America*, *99*, 1389–1394. https://doi.org/10.1073/pnas.012249999

IPCC. (2007). *Climate change 2007: The physical science basis: Contribution of working group I to the fourth assessment report of the Intergovernmental Panel on Climate Change*. Cambridge: Cambridge University Press. ISBN 978 0521 88009-1.

Janssen, P., & Heuberger, P. (1995). Calibration of process-oriented models. *Ecological Modelling*, *83*, 55–66. https://doi.org/10.1016/0304-3800(95)00084-9

Kellndorfer, J., Walker, W., Kirsch, K., Fiske, G., Bishop, J., Lapoint, L., … Westfall, J. (2013). NACP aboveground biomass and carbon baseline data, V. 2 (NBCD 2000), U.S.A., 2000. Data set. Retrieved from http://daac.ornl.gov from ORNL DAAC, Oak Ridge, TN. https://doi.org/10.3334/ORNLDAAC/1161

King, A. W., Andres, R. J., Davis, K. J., Hafer, M., Hayes, D. J., Huntzinger, D. N., … Woodall, C. W. (2015). North America's net terrestrial CO_2 exchange with the atmosphere 1990–2009. *Biogeosciences*, *12*, 399–414. https://doi.org/10.5194/bg-12-399-2015

Landry, J. S., Parrott, L., Price, D. T., Ramankutty, N., & Matthews, H. D. (2016). Modelling long-term impacts of mountain pine beetle outbreaks on merchantable biomass, ecosystem carbon, albedo, and radiative forcing. *Biogeosciences*, *13*, 5277–5295. https://doi.org/10.5194/bg-13-5277-2016

Landry, J. S., Price, D. T., Ramankutty, N., Parrott, L., & Matthews, H. D. (2016). Implementation of a Marauding Insect Module (MIM, version 1.0) in the Integrated Biosphere Simulator (IBIS, version 2.6b4) dynamic vegetation–land surface model. *Geoscientific Model Development*, *9*, 1243–1261. https://doi.org/10.5194/gmd-9-1243-2016

Law, B. E., Hudiburg, T. W., & Luyssaert, S. (2013). Thinning effects on forest productivity: Consequences of preserving old forests and mitigating impacts of fire and drought. *Plant Ecology & Diversity*, *6*, 73–85. https://doi.org/10.1029/2010JG001390

Lindsay, K., Bonan, G. B., Doney, S. C., Hoffman, F. M., Lawrence, D. M., Long, M. C., … Thornton, P. E. (2014). Preindustrial-control and twentieth-century carbon cycle experiments with the earth system model CESM1(BGC). *Journal of Climate*, *27*, 8981–9005. https://doi.org/10.1175/JCLI-D-12-00565.1

Liu, J., Sleeter, B. M., Zhu, Z., Heath, L. S., Tan, Z., Wilson, T. S., … Zhou, D. (2016). Estimating carbon sequestration in the piedmont ecoregion of the United States from 1971 to 2010. *Carbon Balance and Management*, *11*, 1–13. https://doi.org/10.1186/s13021-016-0052-y

Liu, J., Vogelmann, J. E., Zhu, Z., Key, C. H., Sleeter, B. M., Price, D. T., … Jiang, H. (2011). Estimating California ecosystem carbon change using process model and land cover disturbance data: 1951–2000. *Ecological Modelling*, *222*(1), 2333–2341. https://doi.org/10.1016/j.ecolmodel.2011.03.042

Lu, X., Jiang, H., Liu, J., Zhang, X., Jin, J., Zhu, Q., … Peng, C. (2016). Simulated effects of nitrogen saturation on the global carbon budget using the IBIS model. *Scientific Reports*, *6*, 39173. https://doi.org/10.1038/srep39173

Masek, J. G., Cohen, W. B., Leckie, D., Wulder, M. A., Vargas, R., de Jong, B., … Smith, W. B. (2011). Recent rates of forest harvest and conversion in North America. *Journal of Geophysical Research*, *116*, G00K03. https://doi.org/10.1029/2010JG001471

Oswalt, S. N., & Smith, W. B. (2012). US forest resource facts and historical trends. FS-1035. (USDA Forest Service).

Pan, Y., Birdsey, R. A., Fang, J., Houghton, R., Kauppi, P. E., Kurz, W. A., … Hayes, D. (2011). A large and persistent carbon sink in the world's forests. *Science*, *333*, 988–993. https://doi.org/10.1126/science.1201609

Piao, S., Huang, M., Liu, Z., Wang, X., Ciais, P., Canadell, J. G., … Wang, T. (2018). Lower land-use emissions responsible for increased net land carbon sink during the slow warming period. *Nature Geoscience*, *11*(10), 739–743. https://doi.org/10.1038/s41561-018-0204-7

Pugh, T. M. A., Lindeskog, M., Smith, B., Poulter, B., Arneth, A., Haverd, V., & Calle, L. (2019). Role of forest regrowth in global carbon sink dynamics. *Proceedings of the National Academy of Sciences of the United States of America*, *116*(10), 4382–4387. https://doi.org/10.1073/pnas.1810512116

Schimel, D., Sellers, P., Moore III, B., Chatterjee, A., Baker, D., … Yokota, T. (2016). Observing the carbon-climate system. arXiv preprint arXiv:1604.02106.

Sitch, S., Friedlingstein, P., Gruber, N., Jones, S. D., Murray-Tortarolo, G., Ahlström, A., … Myneni, R. (2015). Recent trends and drivers of regional sources and sinks of carbon dioxide. *Biogeosciences*, *12*, 653–679. https://doi.org/10.5194/bg-12-653-2015

Sleeter, B. M., Sohl, T. L., Loveland, T. R., Auch, R. F., Acevedo, W., Drummond, M. A., … Stehman, S. V. (2013). Land-cover change in the conterminous United States from 1973 to 2000. *Global Environmental Change*, *23*, 733–748. https://doi.org/10.1016/j.gloenvcha.2013.03.006

Soil Survey Staff. (2019). Soil Survey Geographic (SSURGO) database. Natural Resources Conservation Service, United States Department of Agriculture. Retrieved from https://websoilsurvey.nrcs.usda.gov/DataAvailability/SoilDataAvailabilityMap.pdf

U.S. Environmental Protection Agency. (2014). Inventory of U.S. greenhouse gas emissions and sinks: 1990-2012. Chapter 7. In *Land use, land-use change, and forestry*. Washington, DC: U.S. Environmental Protection Agency.

U.S. Geological Survey. (2016). Protected areas database of the United States, version 1.4. U.S. Geological Survey Gap Analysis Program database. Retrieved from http://gapanalysis.usgs.gov/padus/

USDA Forest Service. (2016). Forest inventory and analysis national program data and tools. Retrieved from https://www.fia.fs.fed.us/tools-data/index.php

Van Deusen, P., & Heath, L. S. (2016). COLE web applications suite. NCASI and USDA Forest Service. Retrieved from http://www.ncasi2.org/COLE/

Wania, R., Ross, I., & Prentice, I. C. (2009). Integrating peatlands and permafrost into a dynamic global vegetation model: 2. Evaluation and sensitivity of vegetation and carbon cycle processes. *Global Biogeochemical Cycles*, *23*, GB3015. https://doi.org/10.1029/2008GB003413

Węglarczyk, S. (1998). The interdependence and applicability of some statistical quality measures for hydrological models. *Journal of Hydrology*, *206*, 98–103. https://doi.org/10.1016/S0022-1694(98)00094-8

Williams, C. A., Gu, H., MacLean, R., Masek, J. G., & Collatz, J. (2016). Disturbance and the carbon balance of US forests: A quantitative review of impacts from harvests, fires, insects, and droughts. *Global and Planetary Change*, *143*, 66–80. https://doi.org/10.1016/j.gloplacha.2016.06.002

Woodbury, P. B., Smith, J. E., & Heath, L. S. (2007). Carbon sequestration in the U.S. forest sector from 1990 to 2010. *Forest Ecology and Management*, *241*, 14–27. https://doi.org/10.1016/j.foreco.2006.12.008

Xia, J., Luo, Y., Wang, Y. P., Weng, E., & Hararuk, O. (2012). A semi-analytical solution to accelerate spin-up of a coupled carbon and nitrogen land model to steady state. *Geoscientific Model Development*, *5*, 803–836. https://doi.org/10.5194/gmd-5-1259-2012

Yanai, R. D. (1998). The effect of whole-tree harvest on phosphorus cycling in a northern hardwood forest. *Forest Ecology and Management*, *104*, 281–295. https://doi.org/10.1016/S0378-1127(97)00256-9

Zhang, Z., Jiang, H., Liu, J., Zhang, X., Huang, C., Lu, X., … Zhou, G. (2014). An analysis of the global spatial variability of column-averaged CO_2 from SCIAMACHY and its implications for CO_2 sources and sinks. *International Journal of Remote Sensing*, *35*, 2047–2066. https://doi.org/10.1080/01431161.2014.885151

Zhao, M., Heinsch, F. A., Nemani, R. R., & Running, S. W. (2005). Improvements of the MODIS terrestrial gross and net primary production global data set. *Remote Sensing of Environment*, *95*, 164–176. https://doi.org/10.1016/j.rse.2004.12.011

Zhou, D., Liu, S., Oeding, J., & Zhao, S. (2013). Forest cutting and impacts on carbon in the eastern United States. *Scientific Reports*, *3*(1), https://doi.org/10.1038/srep03547

SUPPORTING INFORMATION

Additional supporting information may be found online in the Supporting Information section.

How to cite this article: Liu J, Sleeter BM, Zhu Z, et al. Critical land change information enhances the understanding of carbon balance in the United States. *Glob Change Biol*. 2020;26:3920–3929. https://doi.org/10.1111/gcb.15079